Alkali Cation Extraction by Calix[4]crown-6 to Room-Temperature Ionic Liquids. The Effect of Solvent Anion and Humidity Investigated by Molecular Dynamics Simulations

N. Sieffert and G. Wipff*

Laboratoire MSM, UMR CNRS 7177, Institut de Chimie, 4 rue B. Pascal, 67 000 Strasbourg, France

Received: September 3, 2005; In Final Form: November 3, 2005

We report a molecular dynamics study on the solvation of M^+ (Na^+ to Cs^+) alkali cations and of their $\mathbf{L}M^+$ complexes with a calix[4]arene host (**L** = 1,3-dimethoxy-calix[4]arene-crown-6 in the 1,3-alternate conformation) in the [BMI][PF_6] and [BMI][Tf_2N] room-temperature ionic liquids "ILs" based on the BMI^+ (1-butyl-3-methylimidazolium) cation. The comparison of the two liquids and the dry versus humid form of the former one (with a 1:1 ratio of H_2O and $BMI^+PF_6^-$ species) reveals the importance of humidity: in [BMI][PF_6]-dry as in the [BMI][Tf_2N] liquid, the first solvation shell of the "naked" M^+ ions is composed of solvent anions only (four PF_6^- anions, and from four to five Tf_2N^- anions, respectively, quasi-neutralized by a surrounding cage of BMI^+ cations), while in the [BMI][PF_6]-humid IL, it comprises from one to three solvent anions and about four H_2O molecules. In the $\mathbf{L}M^+$ complexes, the cation is shielded from solvent, but still somewhat interacts with a solvent anion in the dry ILs and with water in the humid IL. We also report tests on M^+ interactions with solvent anions PF_6^- and Tf_2N^- in the gas phase, showing that the AMBER results are in satisfactory agreement with QM results obtained at different levels of theory. The question of ion recognition by **L** is then examined by free energy perturbation studies in the three liquids, predicting a high Cs^+/Na^+ selectivity upon liquid extraction from an aqueous phase, in agreement with experimental results on a parent calixarene host. A similar Cs^+/Na^+ selectivity is predicted upon complexation in a homogeneous IL phase, mainly due to the desolvation energy of the free cations. Thus, despite their polar character, ionic liquids qualitatively behave as classical weakly polar organic liquids (e.g., choroform) as far as liquid−liquid extraction is concerned but more like polar liquids (water, alcohols) as far as complexation in a single phase is concerned.

Introduction

Calix[4]crown-6 calixarenes conformationally locked in the 1,3-alternate conformation by suitable substituents (Figure 1) display outstanding complexation properties toward Cs^+, with a very high binding selectivity toward other alkali cations (hereafter noted M^+). This exceptional affinity for Cs^+ is observed upon complexation in a given homogeneous phase (e.g., methanol, acetonitrile),[1] as well as in liquid−liquid extraction of M^+ from aqueous to organic phases (e.g., halogenated alkanes, aromatic derivatives), allowing for important developments in the context of Cs^+ partitioning from acidic[2,3] or basic[4−9] liquid waste solutions. Recently, room-temperature ionic liquids ("IL"s) have emerged as a new class of "green solvents" for liquid−liquid extraction,[10−13] generally displaying higher extraction efficiency, compared to that of classical organic solvents. They are, by definition, composed of cations (like ammonium, pyridinium, imidazolium derivatives) and anions Y^- and have lower melting points (generally less than 100 °C) compared to those of molten salts. Their miscibility with water and hygroscopic character mainly depend on the choice of Y^-. Typical ILs used in liquid extraction are based on PF_6^- or Tf_2N^- anions and *n*-alkyl-methylimidazolium cations (see Figure 2) and do not mix, at the macroscopic level, with water. Luo et al. found that the BOBCalixC6 (calix[4]-arene-bis(*tert*-octylbenzo-crown-6)) calixarene (see Figure 1) efficiently extracts Cs^+ from aqueous solutions under conditions which give negligible extraction with traditional solvents (e.g., 1,2-dichloroethane or chloroform), with a high selectivity over

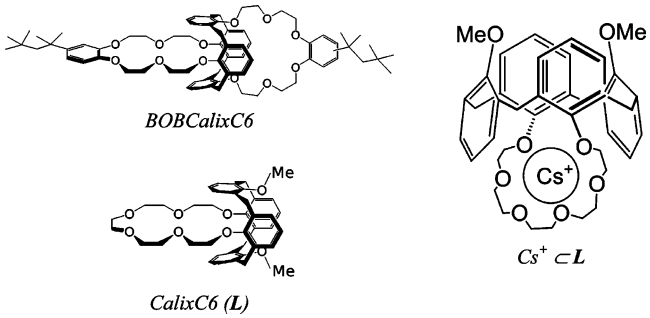

Figure 1. BOBCalixC6, calix[4]crown-6 (**L**) and the $\mathbf{L}Cs^+$ complex.

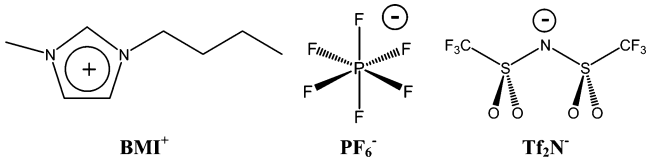

Figure 2. Components of the simulated ionic liquids.

Na^+ or Sr^{2+} cations.[13] Even in the absence of extractant molecule, some partitioning of the "free" Cs^+ cation to the IL phase was observed when the IL is not "too hydrophobic" (i.e., with small alkyl substituents on the imidazolium cation), and this contrasts with classical hydrophobic liquids to which no cation transfer is detected.[12] Another distinguishing feature concerns the extraction mechanism. Whereas upon M^{n+} cation extraction by neutral extractants to classical solvents, the neutrality of the source and receiving phases is retained by coextracting counterions, extraction to ILs may involve a cation

* Corresponding author. E-mail: wipff@chimie.u-strasbg.fr.

10.1021/jp054990s CCC: $33.50
Published on Web 12/21/2005

exchange mechanism (e.g., exchanging M^+ with a solvent cation). Similar features have been observed in the extraction of alkali and Sr^{2+} ions by crown ethers,[10,11,14−16] or in the extraction of hard metallic cations.[17−21] Clearly, solvation plays a key role in liquid−liquid extraction, as well as in ion complexation in solution. So far, little is known, however, on the solvation of simple solutes in ILs. Important insights into the structure of ILs and their interactions with neutral solutes can be obtained by computer simulations. This led our group to undertake molecular dynamics "MD" studies on the solvation of trivalent lanthanide M^{3+}, UO_2^{2+}, and Sr^{2+} cations in pure ILs or in ILs containing "impurities" like water or halide anions.[22−25] The effect of IL humidity on the solvation of 18-crown-6 and its complexes has been also reported.[26]

In this paper, we focus on the question of alkali cation complexation by calixcrowns, choosing 1,3-alternate-dimethoxy-calix[4]arene-crown-6 (**L**) as ligand. The latter is a good mimic of BOBCalixC6 as far as the complexation of Cs^+ is concerned. Furthermore, there are MD results on its alkali complexes in classical solvents,[27−30] as well as on its liquid−liquid extraction[31] and interfacial properties.[31,32] It is thus important to compare these results with those obtained in ionic liquids. Inspired by the liquid−liquid extraction experiments,[13] we selected the [BMI][PF_6] and [BMI][Tf_2N] ionic liquids based on the BMI^+ cation ($BMI^+ \equiv$ *n*-butyl-methylimidazolium) but differing by their anionic component (see Figure 2). The former liquid is more hygroscopic than [BMI][Tf_2N] and, when contacted with water, may contain up to 0.26 molar fraction of water.[33] Water may also be dragged to the IL phase by ligands or complexes. This is why we compare the "dry" vs "humid" forms of [BMI][PF_6]. The humid model contains one H_2O molecule per $BMI^+PF_6^-$ ion pair and is thus oversaturated compared to experiment, whereas the dry [BMI][PF_6] liquid does not contain water at all. These two models should bracket to the "real state" of the IL phase contacted with water. For the more hydrophobic [BMI][Tf_2N] liquid, only the dry form has been considered.

In each liquid, we first investigate the solvation of the different partners involved in alkali cation recognition by the calixcrown: the "naked" cations M^+ (Na^+ to Cs^+), the free ligand **L**, and the $\mathbf{L}M^+$ complexes. Given the lack of experimental reference data concerning the interaction of M^+ ions with solvent anions ($Y^- = PF_6^-$ or Tf_2N^-) in the gas phase, we also investigate various M^+Y^- dimers and aggregates by quantum mechanical "QM" calculations. The crucial question of ion recognition upon complexation and extraction is then examined by using free energy perturbation (FEP) simulations. FEP results will also allow us to gain insights into the relative free energies of transfer of the free M^+ cations from water to the ILs, compared to those of a classical organic solvent like chloroform.

Methods

Molecular Dynamics. The MD simulations were performed with the modified AMBER7.0 software[34] where the potential energy is described by a sum of bond, angle and dihedral deformation energies, and pair wise additive 1−6−12 (electrostatic + van der Waals) interactions between nonbonded atoms.

$$U = \sum_{\text{bonds}} K_r(r - r_{\text{eq}})^2 + \sum_{\text{angles}} K_\theta(\theta - \theta_{\text{eq}})^2 + \sum_{\text{dihedrals}} \sum_n V_n(1 + \cos(n\varphi - \gamma)) + \sum_{i<j} \left(\frac{q_i q_j}{R_{ij}} - 2\epsilon_{ij}\left(\frac{R_{ij}^*}{R_{ij}}\right)^6 + \epsilon_{ij}\left(\frac{R_{ij}^*}{R_{ij}}\right)^{12} \right)$$

TABLE 1: Characteristics of the Simulated Systems

	[BMI][PF_6]-dry		[BMI][PF_6]-humid		[BMI][Tf_2N]-dry	
	no. IL[a]	density[b]	no. IL[a]	density[b]	no. IL[a]	density[b]
Na^+	257	1.32	238	1.31	196	1.49
K^+	257	1.32	238	1.31	195	1.49
Rb^+	257	1.31	238	1.31	194	1.50
Cs^+	257	1.32	238	1.30	194	1.49
L	235	1.32	223	1.31	184	1.48
$\mathbf{L}Na^+$	239	1.31	221	1.29	184	1.49
$\mathbf{L}K^+$	236	1.32	221	1.30	185	1.50
$\mathbf{L}Rb^+$	239	1.31	221	1.30	181	1.49
$\mathbf{L}Cs^+$	235	1.31	220	1.30	184	1.49

[a] Number of ILs ion pairs in the simulation box. [b] Average density of the system.

Cross terms in van der Waals interactions were constructed using the Lorentz−Berthelot rules. The parameters used for the ILs have been tested on the pure ionic liquid properties: those of BMI^+ were taken from de Andrade et al,[35] while those from PF_6^- stem from the OPLS force field[36] and have been used by Margulis et al. to simulate ILs.[37] The corresponding force field parameters have been tested for liquid simulations.[38] The parameters used for Tf_2N^- were from Lopes et al..[39] Water was described by the TIP3P model.[40] Parameters of the Na^+, K^+, Rb^+, and Cs^+ cations were fitted on the hydration free energies by Åqvist,[41] and their interaction with IL anions will be investigated by QM calculations (see section 1 of this paper). The calixarene (**L**) charges and parameters were from ref 31. 1−4 van der Waals interactions were scaled down by a factor of 2, and the corresponding Coulombic interactions were scaled down by 1.2, as recommended by Cornell et al.[42] The systems were represented with 3D periodic boundary conditions. The nonbonded interactions were calculated using a 12 Å atom-based cutoff correcting for the long-range electrostatics using the Ewald summation method (PME approximation),[43,44] except in the case of the free energy perturbation calculations where the direct Ewald summation has been used. The MD simulations were performed at 300 K starting with random velocities. The temperature was monitored by coupling the system to a thermal bath using the Berendsen algorithm[45] with a relaxation time of 0.2 ps. All C−H and O−H bonds were constrained with SHAKE, using the Verlet leapfrog algorithm with a time step of 2 fs to integrate the equations of motion.

Molecular Dynamics. The solutes were initially immersed in cubic boxes of 45 Å length containing the liquid (dry or humid [BMI][PF_6] or dry [BMI][Tf_2N]). The characteristics of the simulated systems are gathered in Table 1. After 1000 steps of energy minimization, the systems were equilibrated by a sequence of (i) 10 ps of dynamics at constant volume with frozen solute (BELLY option of AMBER), (ii) 100 ps of dynamics with frozen solute at a constant pressure of 1 atm, and (iii) 50 ps of dynamics at a constant pressure of 1 atm with free solute in order to fit the experimental densities. In the [BMI][Tf_2N] solution, the relaxation was slower and the last step needed to be increased to 400 ps. All systems were then simulated at constant volume for 2 ns. The MD trajectories were saved every 1 ps and were analyzed using our DRAW and MDS softwares.[46] Typical snapshots have been redrawn with the VMD software.[47]

Analysis of the Trajectories. The average solvation structure was characterized by the radial distribution functions (RDFs) of the P_{PF_6}, F_{PF_6}, $N_{butyl(BMI)}$, O_{H_2O}, H_{H_2O}, N_{Tf_2N}, and O_{Tf_2N} solvent atoms around the M^+ cation during the last 0.5 ns of dynamics. For the free ligand, RDFs were drawn around the center of mass of the six oxygens of the calixarene crown. The average number of coordinated O_{Tf_2N}, O_{H_2O}, F_{PF_6}, $N_{(Butyl)BMI}$ solvent atoms was

TABLE 2: Interaction Energies (kcal/mol) of the $M^+PF_6^-$ and $M^+Tf_2N^-$ Pairs Obtained by QM and by AMBER Optimizations

M^+Y^-	HF 6-31G*	B3LYP 6-31G*	B3LYP cc-pVTZ	AMBER
$Na^+PF_6^-$	−118.5	−123.3	−118.5	−101.2
$K^+PF_6^-$	−102.0	−106.3	−99.9	−92.4
$Rb^+PF_6^-$	−93.1	−94.8	−94.5	−88.6
$Cs^+PF_6^-$	−86.9	−88.2	−88.5	−84.0
$Na^+Tf_2N^-$	−117.9	−122.2	−117.7	−106.4
$K^+Tf_2N^-$	−102.0	−105.0	−99.2	−95.3
$Rb^+Tf_2N^-$	−94.7	−95.9	−93.8	−90.9
$Cs^+Tf_2N^-$	−88.6	−89.4	−87.9	−85.5

calculated by integrating the first peak of the RDF. The number of coordinated anions was similarly extracted from the first peak of the $M-P_{PF_6}$ or $M-N_{Tf_2N}$ RDFs.

Insights into the energy components were obtained by group analysis using a 17 Å cutoff distance and a reaction field correction for the electrostatics. The solute/IL interactions energies were dissected into the contributions of the BMI^+, PF_6^- (or Tf_2N^-), and H_2O molecules. These results were also confirmed by calculations using a 17 Å cutoff and the Ewald summation, therefore requiring charge neutralization of different groups.

Free Energy Calculations. The difference in free energies between two states was obtained using the statistical perturbation theory (FEP) and the windowing technique,[48] with:

$$\Delta G_\lambda = \mathrm{RT} \ln \left\langle \exp \frac{U_\lambda - U_{\lambda+\delta\lambda}}{RT} \right\rangle_\lambda \quad \text{and} \quad \Delta G = \sum \Delta G_\lambda$$

The potential energy U_λ was calculated using a linear combination of the van der Waals parameters of the initial state ($\lambda = 1$) and final state ($\lambda = 0$): $q_\lambda = \lambda q_\lambda + (1 - \lambda) q_0$. The number of intermediate steps ("windows") was 10. At each window, 100 ps of equilibration was followed by 100 ps of data collection for the simulation in the dry and humid [BMI][PF_6]. In the [BMI][Tf_2N] liquid, relaxation is slower, and we performed 200 + 200 ps at each window. The change in ΔG_λ was averaged from the forward and backward cumulated values. Moreover, to avoid as much as possible hysteresis problems, independent simulations were performed from Na^+ to Cs^+ and from Cs^+ to Na^+, via the other cations. For a purpose of comparison, mutations of complexed cations were also performed in the dry [BMI][PF_6] using the thermodynamic integration (TI) technique with 20 windows of 20 + 20 ps.

Quantum Mechanics. The M^+Y^- dimers (M = Na, K, Rb, Cs and Y = PF_6, Tf_2N) and the $Na^+(Y^-)_n$ aggregates ($n = 1-3$) were optimized without any constraints at the Hartree−Fock (HF) and DFT (B3LYP functional) levels of theory, using the Gaussian03 software.[49] Geometries and energies were corrected for basis set superposition errors (BSSEs) using the counterpoise method.[50] Excepted for core electrons of K, Rb, and Cs, the 6-31G* basis set was employed in all systems. Tests with the 6-31+G*, 6-311G*, cc-pVTZ, and lanL2DZ basis sets were also performed on PF_6^-, Tf_2N^-, and their M^+ adducts, showing that the results obtained with the 6-31G* basis set are satisfactory from the energy (see Table 2) as well as from the structural point of view (see Tables S1 and S2 in the Supporting Information). The core electrons of K, Rb, and Cs atoms were described with the effective small core potentials of the Stuttgart group.[51] Insights into electronic effects were obtained by calculating the Mulliken charges (see e.g., Table S3 and S4 in the Supporting Information). The shortcomings of Mulliken population analysis and, in particular, the basis set dependence of resulting charges are well recognized. Relative trends, however, should be described quite faithfully.[52]

Results

We first describe the interactions between the alkali cations ($M^+ = Na^+$, K^+, Rb^+, and Cs^+) and the PF_6^- and Tf_2N^- anions in the gas phase, obtained from QM and molecular mechanics calculations. Then, we analyze the solvation of the free Na^+ and Cs^+ cations, the free calixcrown ligand **L**, and the **L**Na^+ and **L**Cs^+ complexes in the three liquids. The last section deals with the relative free energies of transfer, complexation, and extraction of M^+ cations, obtained by FEP calculations.

1. M^+Y^- (M = Na, K, Rb, or Cs, $Y^- = PF_6^-$ or Tf_2N^-) Pairs and $Na^+(Y^-)_n$ Aggregates in the Gas Phase. We first optimized the $Na^+PF_6^-$, $Na^+Tf_2N^-$, $Cs^+PF_6^-$, and $Cs^+Tf_2N^-$ ions pairs by QM and molecular mechanics (MM) calculations in gas phase, to gain insights into the anions coordination modes and to compare the AMBER to the QM results. As the DFT and HF results follow the same trends, we focus on the former for simplicity. In the optimized $M^+PF_6^-$ complexes, the anion binds tridendate via three F atoms. The Tf_2N^- anion may display several denticities and coordination modes, either via the O atoms from the two SO_2 groups, the N lone pair (see Figure 3), or the CF_3 groups. Optimizations of the $Na^+Tf_2N^-$ and $Cs^+Tf_2N^-$ ion pairs starting from different coordination modes led to different minima, all involving the oxygen atoms of Tf_2N^-. In the most stable ones the two SO_2 groups coordinate bidendate (1 + 1′) or tridendate (2 + 1) to the cation. Bidendate coordination is achieved via one oxygen atom of each $-SO_2$ group, whereas the tridendate coordination involves two oxygens from the one SO_2 group and one oxygen from the second one. These two forms are close in energy ($\Delta E = 0.8$ kcal/mol with Na^+ and 2.8 kcal/mol with Cs^+). With the "softer" Cs^+ cation, another 1 + 1 + 1 form was characterized, where Cs^+ is coordinated to two oxygens (one per SO_2 group) and the N atom. This complex is less stable than the 2 + 1 one by 1.5 kcal/mol. Such 1 + 1 + 1 coordination has been observed in the solid-state structures of Tf_2N^- complexes with metals as Fe^{III} or Ru^{II}, whereas "harder" metals such as Ti^{IV} [53] or trivalent lanthanides cations[54] coordinate the O atoms only. No minimum could be located for the monodendate (via one oxygen) or tetradendate (2 + 2) coordinations which became 2 + 1 or 1 + 1′ during the QM optimizations. When optimized with AMBER, the $Na^+Tf_2N^-$ and $Cs^+Tf_2N^-$ ions pairs systematically converged to a 2 + 1 tricoordination, as found by QM.

$M^+PF_6^-$ and $M^+Tf_2N^-$ pairs with K^+ and Rb^+ cations and tridendate anions were similarly optimized. MM and QM calculated interaction energies (Figure 4, Table 2) show that the smallest and hardest Na^+ cation interacts the best with PF_6^- or Tf_2N^- anions, following the increasing order of cation size ($Na^+ < K^+ < Rb^+ < Cs^+$). Concerning the anion discrimination by M^+, the DFT and HF results show that a given M^+ cation displays quasi-isoenergetic interactions with the Tf_2N^- and PF_6^- anions, the difference generally being ≈1 kcal/mol. The AMBER interaction energies are somewhat smaller, and the QM/AMBER difference decreases from ca. 20 kcal/mol with Na^+ to 4 kcal/mol with Cs^+. AMBER also yields similar interactions of a given M^+ cation with the Tf_2N^- and PF_6^- anions.

The QM results allow us to gain insights into electronic effects, showing that the charge transfer to M^+ and polarization of the anion by M^+ decrease from Na^+ to Cs^+, as expected (Tables S5 and S6 in the Supporting Information). For instance, in both $M^+PF_6^-$ and $M^+Tf_2N^-$ series, the q_M charge ranges from

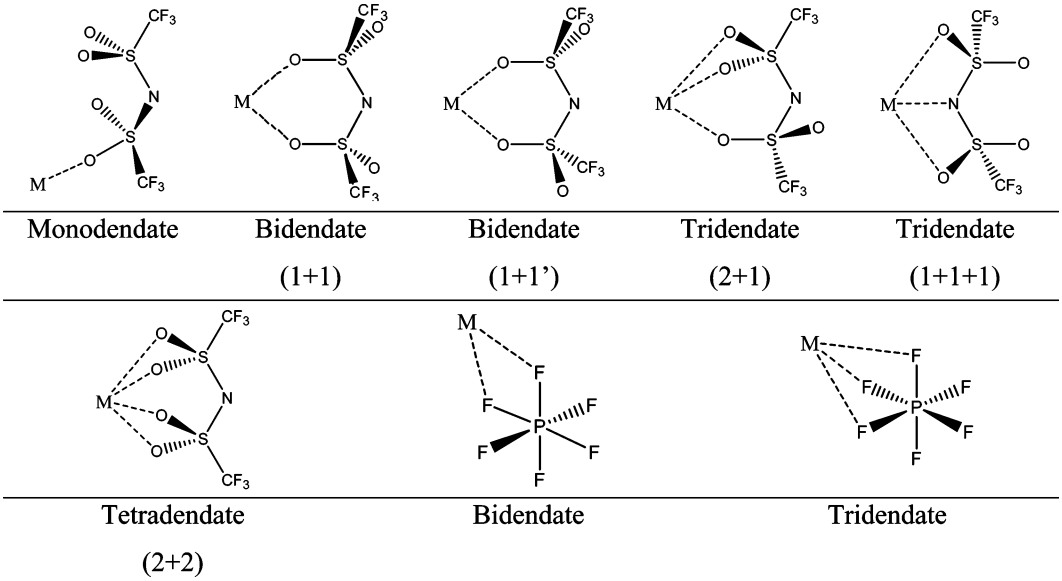

Figure 3. Typical coordination modes of M^+ by Tf_2N^- and PF_6^-.

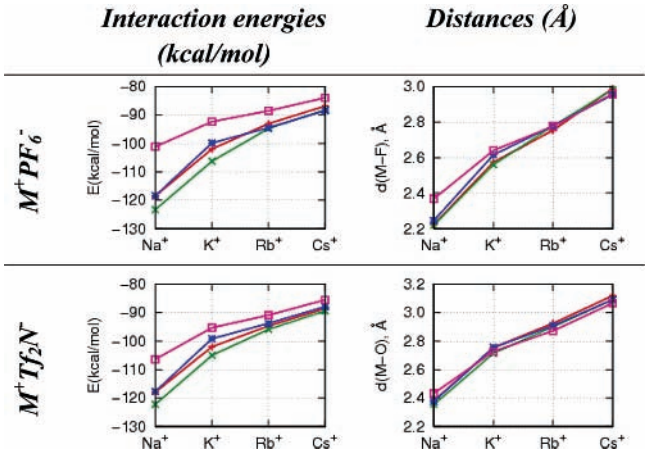

Figure 4. M^+Y^- optimized pairs ($M^+ = Na^+$, K^+, Rb^+, Cs^+ and $Y^- =$ tridendate PF_6^- or 2 + 1 tridendate Tf_2N^-): interaction energies and $M^+-F(PF_6^-)$ and $M^+-O(Tf_2N^-)$ mean distances (Å) from HF/6-31G* (red), DFT(B3LYP)/6-31G* (green), DFT(B3LYP)/cc-pVTZ (blue), and AMBER calculations in the gas phase (purple).

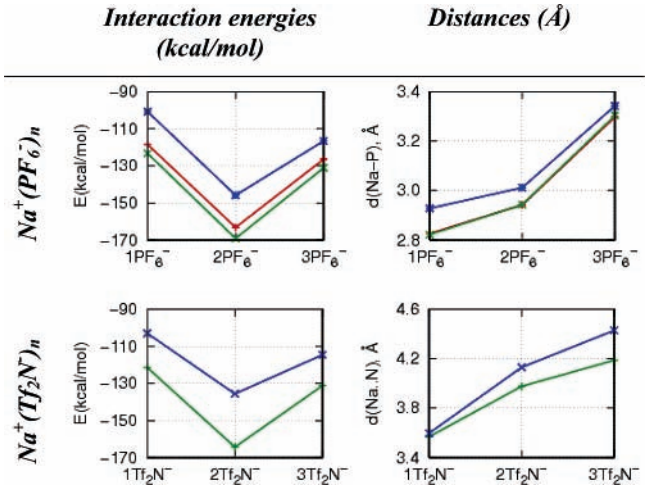

Figure 5. Interaction energies of $Na^+(PF_6^-)_n$ or $Na^+(Tf_2N^-)_n$ complexes ($n = 1-3$) (left) and average $Na^+-P(PF_6^-)$ and $Na^+-N(Tf_2N^-)$ distances (right) from HF/6-31G* (red), DFT/BYL3P/6-31G* (green), and AMBER calculations in the gas phase (blue). $E = E_{Na^+(Y^-)_n} - nE_{Y^-} - E_{Na^+}$.

$\approx +0.5\ e$ for Na^+ to $\approx +0.9\ e$ for Cs^+. Polarization effects can be seen in the $M^+PF_6^-$ complexes in which the q_F charge is $\approx 0.06\ e$ more negative for the coordinated than for the uncoordinated F atoms. For the $M^+Tf_2N^-$ pairs, one can also see some $S^{\delta+}$-$O^{\delta-}$ polarization of the coordinated oxygens, compared to that of the others, and this effect increases with the cation hardness, i.e., from Cs^+ to Na^+ (Table S6 in the Supporting Information).

As in IL solution, the M^+ cation is surrounded by several anions (vide infra), we also investigated higher $Na^+(PF_6^-)_n$ and $Na^+(Tf_2N^-)_n$ aggregates ($n = 2$ and 3) by the QM and MM methods. The energy results are plotted in Figure 5 and summarized in Tables S7 and S8 in the Supporting Information, whereas structural features and electronic charges are gathered in Tables S9 and S10 in the Supporting Information. QM calculations show that the coordination of a second PF_6^- or Tf_2N^- anion ($n = 2$) to the neutral Na^+Y^- species is quite stabilizing (by ≈ -45 kcal/mol), whereas a third one destabilizes the complex (by $\approx +35$ kcal/mol), and these trends are well reproduced with AMBER (-45 and $+29$ kcal/mol, respectively, for the PF_6^- anion and -33 and $+21$ kcal/mol, respectively, for Tf_2N^-). With the three methods, the PF_6^- anions bind tridentate when $n = 1$ or 2, and bidentate when $n = 3$. The binding mode of Tf_2N^- is more versatile and can be either 2 + 1 or 1 + 1, depending on the number of anions and the computational method (see Table S11 in the Supporting Information). As expected, the more ligands, the longer are the $Na-F_{PF_6}$ or $Na-O_{Tf_2N}$ distances, due to ligand−ligand repulsions and the reduced charge of the metal. The Na^+ charge decreases from $+0.59$ to $+0.26\ e$ in the $Na^+(PF_6^-)_n$ series and from $+0.61$ to $+0.36\ e$ in the $Na^+(Tf_2N^-)_n$ series (Tables S9 and S10 in the Supporting Information). Furthermore, the per ligand electron-transfer diminishes in both series (the q_{PF_6} charge decreases from -0.59 to $-0.75\ e$ and the q_{Tf_2N} charge decreases from -0.61 to $-0.79\ e$). Polarization effects also diminish with the increasing number of ligands, as seen, e.g., from the q_F charges of the coordinated versus free F atoms in $Na^+(PF_6^-)_n$. The corresponding Δq_F difference ranges from 0.06 in $Na^+(PF_6^-)$ to only 0.002 e in $Na^+(PF_6^-)_3$. Similar trends are observed on the $Na^+(Tf_2N^-)_n$ aggregates where the charge per Tf_2N^- ranges from $-0.61\ e$ for $Na^+(Tf_2N^-)$ to $-0.79\ e$ for $Na^+(Tf_2N^-)_3$ (Table S10 in the Supporting Information). With the "softer" K^+ to Cs^+ cations, charge transfer and polarization effects

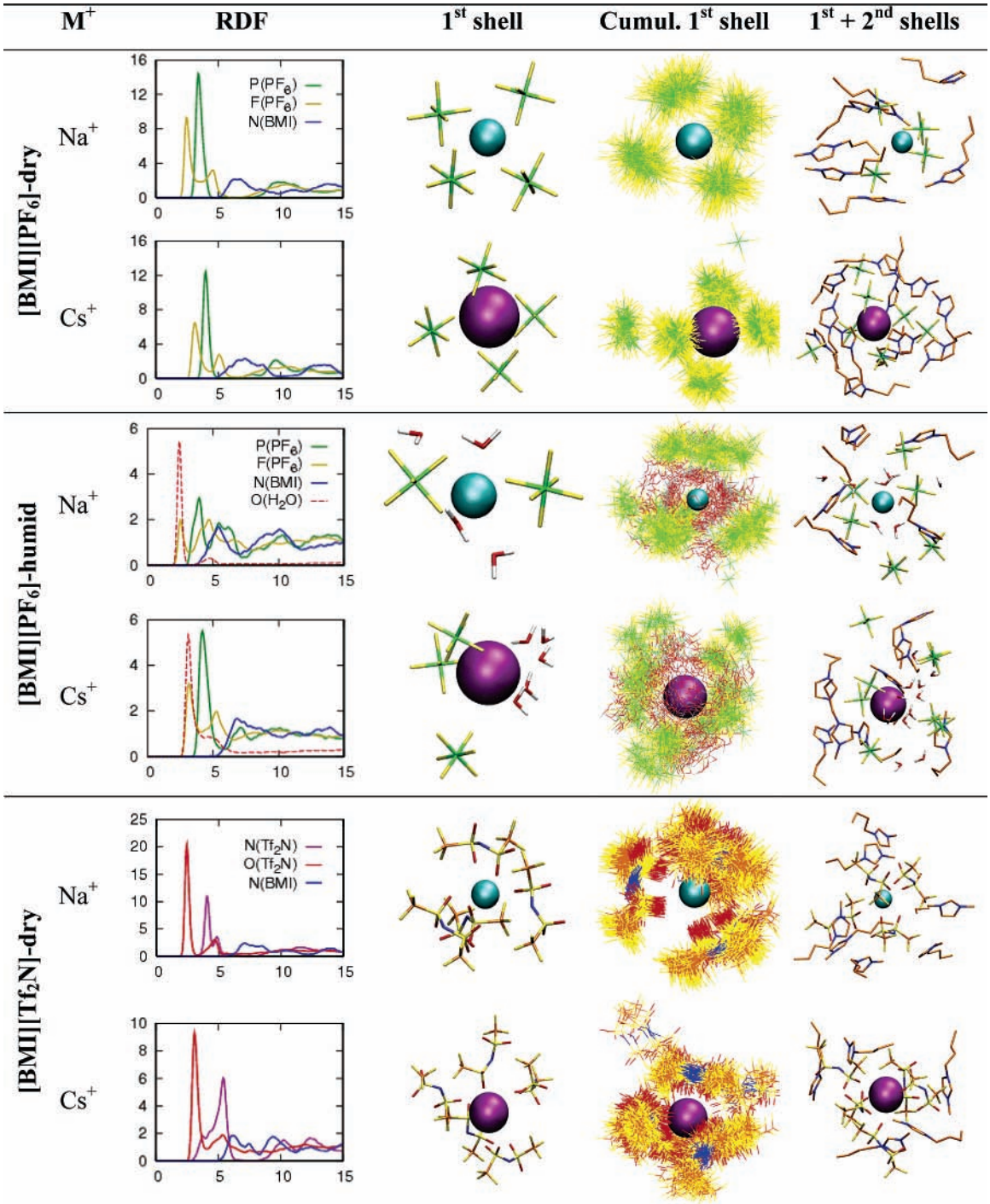

Figure 6. Solvation of free Na^+ and Cs^+ cations in the dry [BMI][PF_6], the humid [BMI][PF_6], and the dry [BMI][Tf_2N]; radial distribution functions of solvent atoms around M^+ (the $M-O(H_2O)$ peaks are scaled down by 10 for Na^+ and by 3 for Cs^+). Cumulated views are shown over the last 0.5 ns of MD selecting anions and water at less than 6 Å from M^+.

should be less important than with Na^+, and the AMBER results in ionic liquid solutions, obtained without dedicated parameter fitting, should be reasonable.

2. Free M^+ Alkali Cations in the Ionic Liquids. In this section, we mainly describe the solvation of the smallest Na^+ and the biggest Cs^+ cations, which bracket the K^+ and Rb^+ ones.

Solvation in Dry [BMI][PF_6]. The first coordination shell of the Na^+ and the Cs^+ cations is composed of four solvent anions which do not exchange with "the bulk" liquid, as shown by the cumulated views taken along the last 0.5 ns of dynamics (see typical snapshots and RDFs in Figure 6 and average coordination numbers of M^+ in Table 3). The integration of the RDFs around Na^+ give 4.0 ± 0.0 P_{PF_6} and 9.7 ± 1.1 F_{PF_6}. This shows that some PF_6^- are bidentate and others are tridentate, on the average. Around the Cs^+ cation, one also finds 4.0 ± 0.0 P_{PF_6} anions but 11.7 ± 0.7 F_{PF_6} atoms, revealing a tridendate coordination of PF_6^-. This first anionic shell is surrounded by a shell of BMI^+ cations (between 5 and 8 Å), and a such alternation of anionic and cationic shells is clearly visible up to 15 Å, as found for di- and trivalent metallic cations.[23,25,55−57]

Solvation in Humid [BMI][PF_6]. As shown by the snapshots and the cumulated views in Figure 6, the presence of water in the IL clearly modifies the first solvation shell of the cation which coordinates water molecules (see Figure 6 and Table 3). The first shell of Na^+ is composed of 1−2 monodentate PF_6^-

TABLE 3: Average Coordination Numbers of M^+ Uncomplexed and Complexed by L[a]

	[BMI][PF_6]-dry		
	P (PF_6)	F (PF_6)	
Na^+	4.0 (0.0)	9.7 (1.1)	
Cs^+	4.0 (0.0)	11.7 (0.7)	
LNa^+	1.0 (0.0)	2.3 (0.5)	
LCs^+	1.0 (0.0)	2.5 (0.6)	
	[BMI][PF_6]-humid		
	P (PF_6)	F (PF_6)	O (H_2O)
Na^+	1.3 (0.6)	1.5 (1.0)	4.3 (0.7)
Cs^+	3.0 (0.4)	5.8 (1.5)	4.4 (1.2)
LNa^+	1.0 (0.1)	1.4 (0.7)	1.0 (0.0)
LCs^+	0.9 (0.4)	*b*	1.0 (0.2)
	[BMI][Tf_2N]-dry		
	N (Tf_2N)	O (Tf_2N)	
Na^+	4.0 (0.1)	5.7 (0.5)	
Cs^+	5.0 (0.2)	6.2 (1.0)	
LNa^+	1.0 (0.3)	0.8 (0.4)	
LCs^+	1.0 (0.0)	1.1 (0.4)	

[a] The rms fluctuations are in parentheses. [b] Not reported because the first peak is ill defined. A full version of this table is given in the Supporting Information (Table S12).

anions plus 4 H_2O molecules "mixed" around the cation. In the case of the bigger Cs^+ cation, it is composed of 3 bidentate PF_6^- anions on one side and 4−5 H_2O molecules on the other side and is thus somewhat "anisotropic". The second solvent shell of Na^+ to Cs^+ ions is mainly composed of BMI^+ cations.

Solvation in Dry [BMI][Tf_2N]. In the [BMI][Tf_2N] liquid, the M^+ cations are fully surrounded by Tf_2N^- anions (see Figure 6 and Table 3) coordinated mono-, bi-, or tridentate via their oxygen atoms. Na^+ is surrounded by 4.0 ± 0.1 N and 5.7 ± 0.5 O atoms, respectively, corresponding to two bidentate plus two monodentate Tf_2N^- anions. The Cs^+ cation is coordinated to 5 Tf_2N^- anions via 6.2 ± 1.0 oxygens on the average, one anion being bidendate (1 + 1) and the others being monodendate.

Interactions of M^+ with the Solvents. The energy component analysis (see Table 4) shows that M^+ cations display strong attractive interactions with the three studied solvents, stemming from the anions contributions, whereas the M^+/BMI^+ interactions are repulsive. Moreover, Na^+ interacts better than Cs^+ with the solvent, by about 43 kcal/mol in the dry [BMI][PF_6] and 50 kcal/mol in the humid [BMI][PF_6] and dry [BMI][Tf_2N] solvents. If one compares a given M^+ cation in the [BMI][PF_6] versus [BMI][Tf_2N] solvents, one sees that it interacts more with the PF_6^- than with the Tf_2N^- anions, by 110−120 kcal/mol in the case of Na^+ and Cs^+. This may appear quite surprising if one considers that M^+ is surrounded by a similar number of solvent anions in solution and displays, in the gas phase, quasi-identical interaction energies with PF_6^- and Tf_2N^-. The difference in solution can be understood from the fact that the Tf_2N^- anions optimally bind to M^+ only in restricted conformations and orientations, whereas the more symmetrical PF_6^- anions statistically display better interactions with M^+. These are, however, compensated by the M^+/BMI^+ repulsions, which are stronger in the [BMI][PF_6] than in the [BMI][Tf_2N] solution.

3. Free Calix[4]crown-6 (L) in the Ionic Liquids. *Solvation in Dry [BMI][PF_6].* As **L** is a neutral species and of low symmetry it does not induce a strong organization of the solvent, making it difficult to recognize a first solvation shell (see Figure 7). Interesting interactions are however observed with the BMI^+ cations which make "facial complexes" with the crown ether moiety or π-interactions with phenyl groups of **L**. In the dry [BMI][PF_6], there is one BMI^+ on each side of the crown, at 3.5 and 5.5 Å, respectively, from its center. Such solvation is reminiscent of what has been observed with 18-crown-6 in [BMI][PF_6] solution.[26] At the periphery of the calixarene, solvent anions and cations are "mixed", as in the bulk liquid.

Solvation in Humid [BMI][PF_6]. The presence of water in the [BMI][PF_6] liquid seems to have little influence on the PF_6^- and BMI^+ organization around the calixarene (see Figure 7). Indeed, although no direct BMI^+ "coordination" to **L** is observed, three BMI^+ are located around the crown, and two others interact via π-stacking interactions with the aromatic skelton. Moreover, no water molecule coordinates the crown, contrary to what is observed in pure water or at the water/chloroform interface.[32] This is probably due to the competitive H-bonds between water and F_{PF_6} atoms. Nevertheless, one finds one H_2O molecule bridging over the two methoxy groups.

Solvation in Dry [BMI][Tf_2N]. In the dry [BMI][Tf_2N], the calixarene is solvated by a mixture of anions and cations, without

TABLE 4: Solvation in ILs: Average Interaction Energies and rms Fluctuations (kcal/mol) between the Solute and the Solvent Components

	BMI^+	Y^-	H_2O	E_{BMI^+}[a]	E_{Y^-}[a]	E_{H_2O}[a]	E_{tot}[a]	$E_{tot/Ewald}$[b]
				[BMI][PF_6]-dry				
Na^+	BMI^+	PF_6^-		489 (9)	−634 (8)		−145 (7)	−148 (7)
Cs^+	BMI^+	PF_6^-		493(8)	−596 (8)		−103 (5)	−105 (6)
L	BMI^+	PF_6^-		−33 (3)	−74 (2)		−107 (4)	−106 (4)
LNa^+	BMI^+	PF_6^-		394 (5)	−540 (8)		−146 (5)	−148 (6)
LCs^+	BMI^+	PF_6^-		385 (6)	−514 (8)		−129 (6)	−131 (6)
				[BMI][PF_6]-humid				
Na^+	BMI^+	PF_6^-	H_2O	457 (16)	−533 (23)	−90 (14)	−167 (9)	−168 (9)
Cs^+	BMI^+	PF_6^-	H_2O	462 (9)	−546 (12)	−33 (10)	−117 (8)	−118 (8)
L	BMI^+	PF_6^-	H_2O	−25 (3)	−60 (3)	−16 (3)	−100 (4)	−100 (4)
LNa^+	BMI^+	PF_6^-	H_2O	348 (5)	−446 (8)	−38 (6)	−136 (6)	−137 (6)
LCs^+	BMI^+	PF_6^-	H_2O	353 (6)	−459 (9)	−19 (5)	−125 (7)	−125 (6)
				[BMI][Tf_2N]-dry				
Na^+	BMI^+	Tf_2N^-		354 (7)	−510 (11)		−156 (10)	−158 (10)
Cs^+	BMI^+	Tf_2N^-		375 (7)	−481 (9)		−106 (7)	−107 (7)
L	BMI^+	Tf_2N^-		−22 (3)	−64 (3)		−86 (4)	−86 (4)
LNa^+	BMI^+	Tf_2N^-		272 (5)	−411 (10)		−139 (8)	−140 (8)
LCs^+	BMI^+	Tf_2N^-		289 (5)	−425 (7)		−136 (6)	−137 (5)

[a] Calculated with a 17 Å cutoff + reaction field correction. [b] Calculated with a 17 Å cutoff + Ewald correction. Averages over the last 0.5 ns of MD.

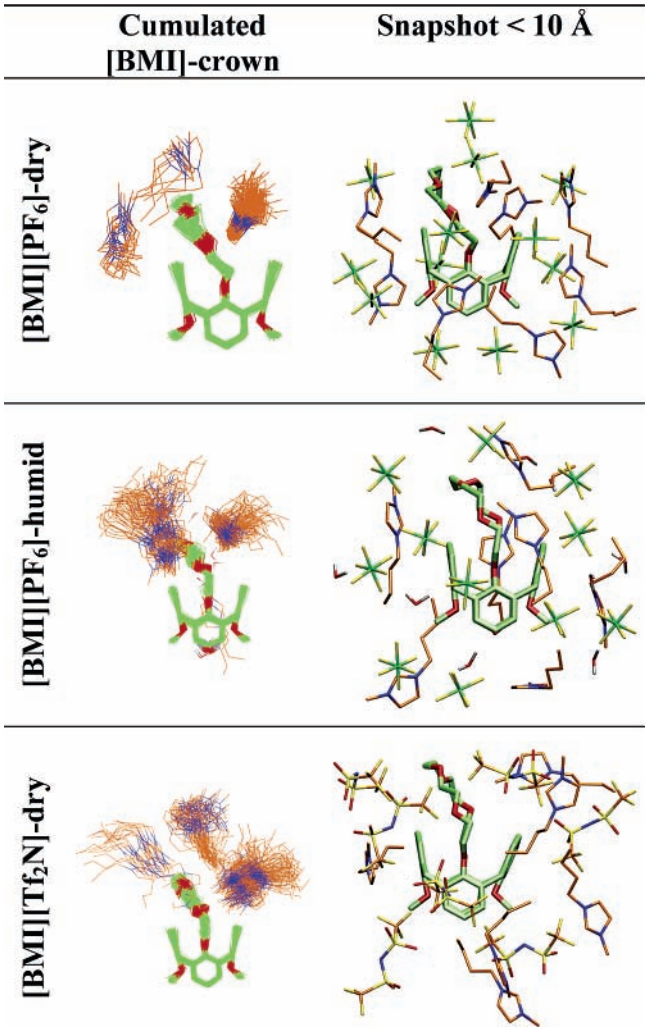

Figure 7. Solvation of free calixarene (**L**) in the dry [BMI][PF_6], the humid [BMI][PF_6], and the dry [BMI][Tf_2N]. Cumulated views are plotted over the last 0.5 ns of MD selecting cations within 6 Å from the center of the crown. A full version of this figure is given in the Supporting Information (Figure S1).

clear organization (see Figure 7). The snapshot of the solvation shell up to 10 Å shows that one BMI^+ cation stacks with an aryl group of **L**. The Tf_2N^- anions, like the PF_6^-, have no specific interactions with the solute.

4. The $M^+ \subset$ Calix[4]crown-6 Complexes in the Ionic Liquids. In the three ILs, the $M^+ \subset$ Calix[4]crown-6 (**L**M^+) complexes remain associated during the dynamics, and the average position of the cation in the host depends on its size. The structure of the **L**Cs^+ complex is similar to the solid-state structure,[1] i.e., Cs^+ sits on the top on the crown with average M^+-O_{crown} distances between 3.17 and 4.94 Å in [BMI][PF_6]. As the crown is somewhat "bent", the complex is more of C_2 than of C_{2v}-type symmetry. **L**Rb^+ and **L**K^+ adopt a similar structure, but Na^+ is too small for this host and, depending on the liquid and simulation conditions, adopts two main modes of binding: either "exo" (i.e., mainly coordinated to the crown oxygens completed by solvent species) or "endo" (coordinated to two oxygens of the crown and to the phenoxy groups of **L**). Although the cations are shielded from solvent, they display specific interactions with a few solvent anions or water molecules.

Solvation in Dry [BMI][PF_6]. The first coordination shell of each complexed cation is composed of the crown ether oxygens, completed by one PF_6^- solvent anion (see Figure 8 and Table 3). The P_{PF_6} coordination number is 1.0 ± 0.0 for both Na^+ (in the exo configuration) and Cs^+ cations, corresponding to 2.3 ± 0.5 and 2.5 ± 0.6 coordinated F_{PF_6} atoms, respectively. This indicates that the PF_6^- anion oscillates between bi- and tridentate coordinations along the dynamics. The first solvation shell is followed by a mixture of solvent cations and anions, without well-defined organization.

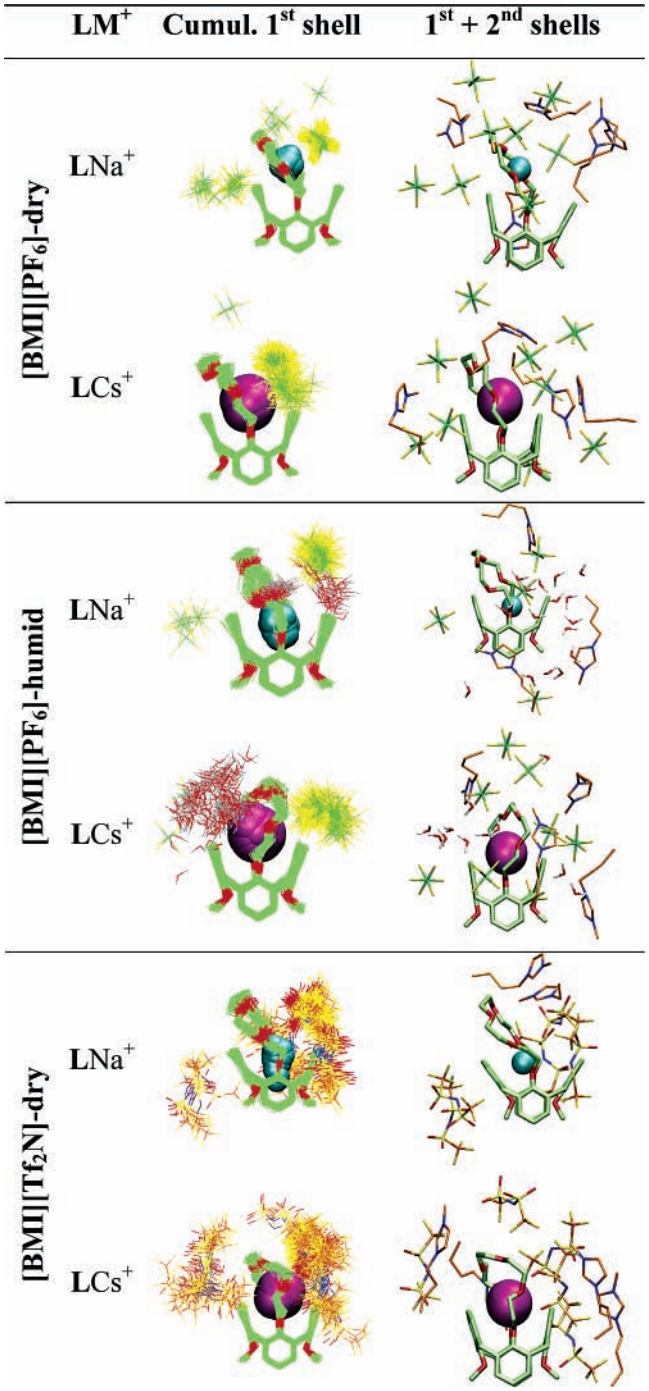

Figure 8. Solvation of the **L**Na^+ and **L**Cs^+ complexes in the dry [BMI][PF_6], the humid [BMI][PF_6], and the dry [BMI][Tf_2N]. Cumulated views are plotted over the last 0.5 ns of MD selecting anions and water within 6 Å from cations. A full version of this figure is given in the Supporting Information (Figure S2).

Solvation in Humid [BMI][PF_6]. In the humid [BMI][PF_6] liquid, the complexed cations are mainly solvated by PF_6^- anions and water. In the case of **L**Na^+ one H_2O molecule is cocomplexed with Na^+, and different configurations are observed (Figure 8 and Table 3), where the cation is either "endo"

TABLE 5: Free Energy Differences (kcal/mol) for "Free" Cations ($\Delta G_{3/IL}$) and Complexed Cations ($\Delta G_{4/IL}$)[a]

mutation	$Na^+ \rightarrow K^+$	$K^+ \rightarrow Rb^+$	$Rb^+ \rightarrow Cs^+$	$Na^+ \rightarrow Cs^+$ [b]
	"Free" Cations in Water ($\Delta G_{3/wat}$)[c]			
water	18.4	5.4	7.8	31.6
	"Free" Cations in ILs ($\Delta G_{3/IL}$)			
[BMI][PF_6]-dry	13.3 (1.7)	6.0 (0.0)	8.0 (0.2)	27.3 (1.9)
FEP	−12.1 (1.5)	−5.9 (0.0)	−7.9 (0.1)	−25.9 (1.6)
	12.7 (1.6)	6.0 (0.0)	8.0 (0.2)	**26.7 (1.8)**
[BMI][PF_6]-humid	17.0 (2.5)	7.1 (0.1)	8.1 (0.3)	32.2 (2.9)
FEP	−16.1 (2.2)	−7.0 (0.1)	−8.0 (0.2)	−31.1 (2.5)
	16.6 (2.3)	7.1 (0.1)	8.1 (0.3)	**31.8 (2.7)**
[BMI][Tf_2N]-dry	17.4 (2.1)	7.0 (0.1)	7.2 (0.2)	31.6 (2.4)
FEP	−17.1 (2.1)	5.8 (0.1)	−8.6 (0.2)	−31.5 (2.4)
	17.3 (2.1)	6.4 (0.1)	7.9 (0.2)	**31.6 (2.4)**
	Complexed Cations in ILs ($\Delta G_{4/IL}$)			
[BMI][PF_6]-dry	10.9 (1.2)	4.8 (0.0)	6.9 (0.0)	22.6 (1.2)
FEP	−10.6 (1.2)	−4.5 (0.0)	−5.8 (0.0)	−20.9 (1.2)
	10.8 (1.2)	4.7 (0.0)	6.4 (0.0)	**21.9 (1.2)**
[BMI][PF_6]-dry	10.7	4.4	6.2	21.3
TI	−9.5	−3.9	−5.8	−19.2
	10.1	4.2	6.0	**20.3**
[BMI][PF_6]-humid	13.3 (1.5)	5.0 (0.0)	7.0 (0.0)	25.3 (1.5)
FEP	−16.5 (1.9)	−5.3 (0.0)	−8.3 (0.0)	30.1 (1.9)
	14.9 (1.7)	5.2 (0.0)	7.7 (0.0)	**27.7 (1.7)**
[BMI][Tf_2N]-dry	10.9 (1.0)	4.6 (0.0)	7.0 (0.1)	22.5 (1.1)
FEP	−9.4 (0.9)	−5.0 (0.0)	−6.5 (0.1)	−20.9 (1.0)
	10.2 (1.0)	4.8 (0.0)	6.8 (0.1)	**21.8 (1.1)**

[a] First line: direct mutation; second line: reversed mutation; third line: average energy. [b] $\Delta G_{(Na^+\rightarrow Cs^+)} = \Delta G_{(Na^+\rightarrow K^+)} + \Delta G_{(K^+\rightarrow Rb^+)} + \Delta G_{(Rb^+\rightarrow Cs^+)}$. [c] Experimental values are from ref 58. See Schemes 1−3 for definitions of $\Delta G_{3/IL}$ and $\Delta G_{4/IL}$. The numbers in parentheses are the differences between the forward and backward cumulated energies.

(with the H_2O molecule on the top), or "exo" (with the H_2O molecule at the bottom). These two configurations have already been characterized in water[28] and are quite specific to the small Na^+ cation. The "endo" configuration also favors π-interactions between Na^+ and the aromatic groups of the calixarene. Cs^+ is too big to cocomplex a H_2O molecule but coordinates one water molecule H-bonded to solvent anions. The first solvation shell of Cs^+ is also completed by one PF_6^- anion. Interestingly, the cation drags water around the complex, as shown by the O_{water} RDF peak. After integration within 10 Å, one finds 18.4 O_{H_2O} around the complexed Na^+ and 11.4 O_{H_2O} around the complexed Cs^+.

Solvation in Dry [BMI][Tf_2N]. In the dry [BMI][Tf_2N], both complexed Na^+ (in the endo configuration) and Cs^+ cations are coordinated to one oxygen atom of a monodendate Tf_2N^- (see Figure 8 and Table 3). The steric hindrance from **L** seems to prevent a bidentate coordination of the anion.

5. Difference in Free Energies in the Ionic Liquids. In this section, we present the results of the mutations of the free and complexed cations in the three liquids. The primary results ("alchemical transformations") are presented in Table 5 and Figure 9. The calculation of the relative free energies of complexation in a given liquid, of M^+ transfer from water to the IL, and of liquid−liquid extraction of M^+ by the calixarene **L** have been based on the thermodynamic cycles (Schemes 1−3 comparing Na^+/Cs^+, as a purpose of illustration), and the results are summarized in Table 6 and in Figure 10.

Relative Free Energies of Solvation of the "Free" Cations ($\Delta G_{3/IL}$). According to FEP calculations, Na^+ is the best solvated cation, and the cation order is $Na^+ > K^+ > Rb^+ > Cs^+$ in the three liquids. The Cs^+/Na^+ free energy difference $\Delta G_{3/IL}$ is quite important (from 26.7 to 31.8 kcal/mol, depending on the liquid) and is mainly due to the K^+/Na^+ contribution. In the case of the $K^+ \leftrightarrow Rb^+$ and $Rb^+ \leftrightarrow Cs^+$ mutations, the calculated $\Delta G_{3/IL}$ values are similar in the three liquids, but for the $Na^+ \leftrightarrow K^+$ mutations $\Delta G_{3/IL}$ is about 4 kcal/mol smaller in the dry than in the humid [BMI][PF_6] and in the dry [BMI][Tf_2N] liquid.

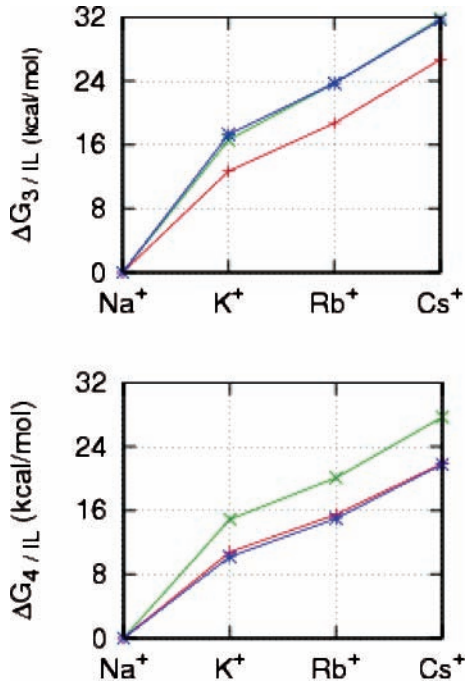

Figure 9. Calculated $\Delta G_{3/IL}$ and $\Delta G_{4/IL}$ free energies in dry [BMI][PF_6] (red), humid [BMI][PF_6] (green), and dry [BMI][Tf_2N] (blue).

Relative Free Energies of the Calixarene Complexes ($\Delta G_{4/IL}$). The differences in free energies obtained for the complexed cations ($\Delta G_{4/IL}$) follow the same trends as for the "free" cations (**L**$Na^+ >$ **L**$K^+ >$ **L**$Rb^+ >$ **L**Cs^+) in the three solutions. Moreover, the Cs^+/Na^+ difference is similar in the two dry ILs (22 kcal/mol) but increases in the humid [BMI][PF_6] (28 kcal/mol) (see Table 5). Note that in the case of the $Na^+ \rightarrow K^+$ mutation, the cocomplexation of one water molecule by **L** caused sampling problems, related to the fact that the "exo" and "endo" (see section 4) configurations did not exchange during the dynamics and yielded to distinct $\Delta G_{4/IL}$'s. Thus, several independent $Na^+ \rightarrow K^+$ and $K^+ \rightarrow Na^+$ mutation simulations have been performed with different sampling conditions, yielding $\Delta G_{4/IL}$ values ranging from 12.9 to 16.4 kcal/mol (See Figure S3 in the Supporting Information), with a hysteresis of ≈2 kcal/mol. This is why an average value of 14.9 kcal/mol has been used for subsequent calculations. The mutations of complexed cations performed in the dry [BMI][PF_6] using the thermodynamic integration (TI) method support the FEP results, as similar $\Delta G_{4/IL}$ values are obtained by the two methods.

Complexation Selectivities in the Ionic Liquids ($\Delta\Delta G_c$). The binding selectivity ($\Delta\Delta G_c$) between two cations in a given liquid, defined by $\Delta\Delta G_c = \Delta G_{c1} - \Delta G_{c2}$, was calculated as the difference between $\Delta G_{3/IL}$ and $\Delta G_{4/IL}$ ($\Delta\Delta G_c = \Delta G_{c1} - \Delta G_{c2} = \Delta G_{3/IL} - \Delta G_{4/IL}$) following the "alchemical" route (Scheme 1).

The results show that **L** complexes selectively Cs^+, following the order $Cs^+ > Rb^+ > K^+ > Na^+$ in the three studied ILs. The Cs^+/Na^+ binding selectivity $\Delta\Delta G_c$ amounts to 4.8 kcal/mol in the dry [BMI][PF_6], 3.9 kcal/mol in the humid [BMI][PF_6], and 9.8 kcal/mol in [BMI][Tf_2N]. It is thus highest in the most hydrophobic liquid. In dry and humid [BMI][PF_6], the K^+/Na^+, Rb^+/K^+, and Cs^+/Rb^+ contributions are very similar

TABLE 6: Free Energy Differences for Cation Complexation ($\Delta\Delta G_c$), Cation Transfer from Water to ILs (without L) ($\Delta\Delta G_t$), and Cation Extraction from Water to ILs (by L) ($\Delta\Delta G_e$) Obtained by FEP Calculations

		$Na^+ \rightarrow K^+$	$K^+ \rightarrow Rb^+$	$Rb^+ \rightarrow Cs^+$	$Na^+ \rightarrow Cs^+$ [a]
		M^+ complexation by **L** in ILs (Scheme 1)			
[BMI][PF_6]-dry	$\Delta\Delta G_c$	1.9	1.3	1.6	**4.8**
[BMI][PF_6]-humid	$\Delta\Delta G_c$	1.7	1.9	0.3	**3.9**
[BMI][Tf_2N]-dry	$\Delta\Delta G_c$	7.1	1.6	1.1	**9.8**
		M^+ transfer from water to ILs (without **L**) (Scheme 2)			
[BMI][PF_6]-dry	$\Delta\Delta G_t$	5.7	−0.6	−0.2	**4.9**
[BMI][PF_6]-humid	$\Delta\Delta G_t$	1.8	−1.8	−0.2	**−0.2**
[BMI][Tf_2N]-dry	$\Delta\Delta G_t$	1.1	−1.0	−0.1	**0.0**
		M^+ extraction from water to ILs (by **L**) (Scheme 3)			
[BMI][PF_6]-dry	$\Delta\Delta G_e$	7.6	0.7	1.4	**9.7**
[BMI][PF_6]-humid	$\Delta\Delta G_e$	4.1	0.2	0.1	**4.4**
[BMI][Tf_2N]-dry	$\Delta\Delta G_e$	8.2	0.6	1.0	**9.8**

[a] $\Delta G_{(Na^+ \rightarrow Cs^+)} = \Delta G_{(Na^+ \rightarrow K^+)} + \Delta G_{(K^+ \rightarrow Rb^+)} + \Delta G_{(Rb^+ \rightarrow Cs^+)}$.

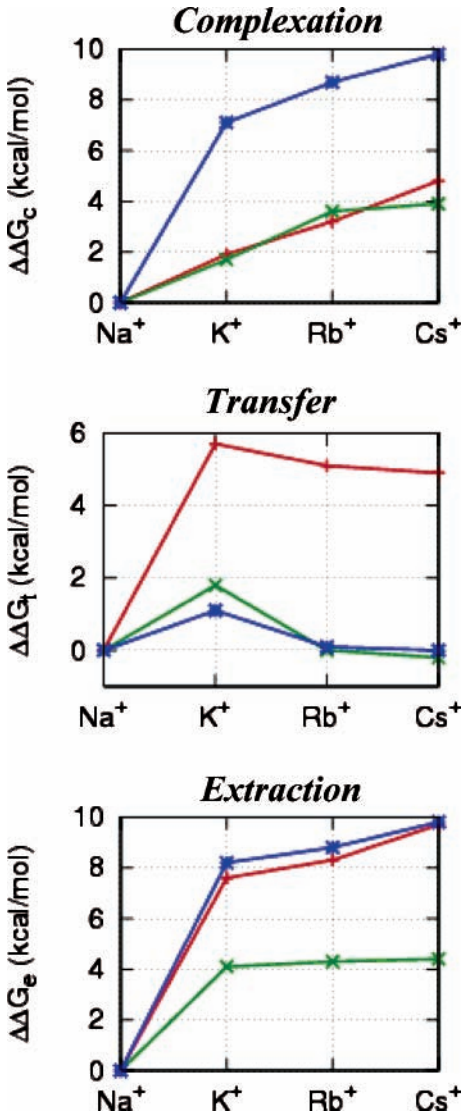

Figure 10. Relative free energies of complexation, transfer, and extraction in dry [BMI][PF_6] (red), humid [BMI][PF_6] (green), and dry [BMI][Tf_2N] (blue).

(about 1.5 kcal/mol), while in [BMI][Tf_2N] the Cs^+/Na^+ binding selectivity mainly stems from the K^+/Na^+ contribution (7.1 kcal/mol).

Transfer of Free Alkali Cations from Water to Ionic Liquids ($\Delta\Delta G_t$). The relative free energies of transfer ($\Delta\Delta G_t$) of two uncomplexed M^+ cations from water to a given ionic liquid was calculated by the difference between $\Delta G_{3/wat}$ and $\Delta G_{3/IL}$ (see Scheme 2): $\Delta\Delta G_t = \Delta G_{t1} - \Delta G_{t2} = \Delta G_{3/wat} - \Delta G_{3/IL}$. The $\Delta G_{3/wat}$ energies are the experimental values from ref 58.

SCHEME 1

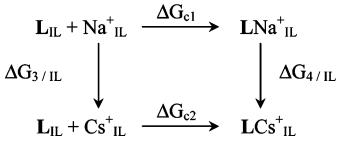

SCHEME 2

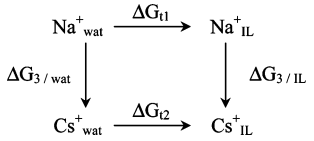

SCHEME 3

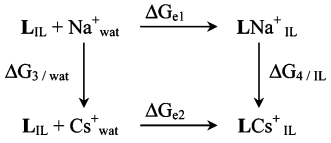

For the Cs^+/Na^+ transfer (see Table 6), $\Delta\Delta G_t$ is positive (4.9 kcal/mol) in the dry [BMI][PF_6]] and nearly zero in the two other liquids, indicating a higher partitioning of Cs^+, compared to that of Na^+, to the [BMI][PF_6] ionic liquid.

Cation Extraction Selectivity from Water to Ionic Liquids ($\Delta\Delta G_e$). The differences in free energy of M^+ extraction by **L** from water to the ionic liquid were similarly calculated by differences between $\Delta G_{3/wat}$ and $\Delta G_{4/IL}$ ($\Delta\Delta G_e = \Delta G_{e1} - \Delta G_{e2} = \Delta G_{3/wat} - \Delta G_{4/IL}$) (Scheme 3).

The $\Delta\Delta G_e$ values (Table 6) reveal a high Cs^+/Na^+ extraction selectivity by **L** in the three ILs. Cs^+ is preferred by 9.7 kcal/mol in the dry [BMI][PF_6] and by 9.8 kcal/mol in the dry [BMI][Tf_2N]. In the humid [BMI][PF_6], the selectivity is reduced to about 4.4 kcal/mol, on the average. In the three ILs the Cs^+/Na^+ extraction selectivity is mainly due to a high K^+/Na^+ contribution, which accounts for about 80% of the Cs^+/Na^+ $\Delta\Delta G_e$ values. The Cs^+/K^+ and Cs^+/Rb^+ extraction selectivities are smaller (between 0.1 and 1.4 kcal/mol), indicating that K^+ and Rb^+ should be coextracted along with Cs^+.

Discussion

We report a MD study on the solvation of several species involved in liquid−liquid extraction of alkali ions to ionic liquids and an FEP study of their relative free energies of transfer,

complexation, and extraction. The MD simulations are based on a simple force field representation of the potential energy of the system, assuming that intermolecular interactions are essentially steric + electrostatic in nature, thus following most current methodologies used to simulate ILs[19,35,39,59−66] or molten salts.[67−70] There is certainly room for methodological improvements including, e.g., charge transfer + polarization effects, but the comparison of QM versus force field results presented here, as well as comparisons involving IL solvent ions or halide complexes of hard (e.g., trivalent lanthanides or uranyl) metallic cations,[23−25,57] shows satisfactory agreement, especially when the cation gets more saturated. This is consistent with the fitting of M^+ parameters in a condensed phase (aqueous solution),[41] instead of using, e.g., $M^+(OH_2)_n$ aggregates.

Cation Solvation in Ionic Liquids, Compared to "Traditional" Solvents. The solute−solvent interactions energies and the FEP results show that the Na^+ cation is better solvated than Cs^+ in the three studied liquids, following the same trends as in dipolar solvents such as water, methanol, DMSO, and acetonitrile.[58] However, the solvation patterns are in many respects quite different. Typically, in classical solvents, the first solvation shells of M^+ are built from the solvent dipoles interacting with M^+ and can be, to a first approximation, described by a gas-phase approach. The solvation in dry ionic liquids differs since the first shell of M^+ is fully anionic in nature and is embedded in a positively charged "cage" of BMI^+ solvent cations, leading to an onion-type alternation of BMI^+ and Y^- solvent ions. As a result, the first shell of M^+ contains more anions (four to five around Na^+ to Cs^+) in solution than in the gas phase, where only two anions should coordinate to M^+. Intrinsically, $Na^+(PF_6^-)_3$ is indeed predicted to be unstable toward the dissociation of one anion, as the third PF_6^- ligand is repulsed by the negatively charged $Na(PF_6)_2^-$ complex. Similar features have been found in the case of, e.g., $EuCl_6^{3-}$ or $UO_2Cl_4^-$ complexes which are stable in ionic liquids or in crystals but not in the gas phase.[23] It is thus essential to consider the second shell and more remote solvent interactions to predict the solvation of ions in ionic liquids. It can also be surmised that the status of counterions is quite different in the ionic liquids, compared to that in conventional solvents. Another difference concerns the coordination number of Na^+ and Cs^+ which is nearly the same in the IL but increases from about 6 to 9 in water.

The comparison of the two dry solvents shows that the PF_6^- and Tf_2N^- anions have similar coordination properties to M^+. The number of coordinated anions ranges from four to five, and the number of coordinated atoms ($F_{PF_6^-}$ or $O_{Tf_2N^-}$) increases with the size of M^+. Nevertheless, the dynamic behavior of the anions somewhat differs, as PF_6^- is coordinated via two or three dynamically exchanging F atoms, whereas Tf_2N^- retains a more fixed coordination mode during the dynamics, anchored by its $-SO_2$ oxygens. Most Tf_2N^- anions bind in a bidentate fashion, but some are monodendate to complete the first coordination shell of M^+ in solution.

Concerning the differences in solvation free energies of M^+, they are predicted to follow the same trends in ionic liquids as in dipolar solvents and water, as predicted by the simple Born solvation model.[71] They are also very close to each other in the three studied liquids. Thus, despite their hydrophobic character, the studied ionic liquids behave like traditional polar solvents.

Another issue concerns the interactions with water. The [BMI][Tf_2N] liquid is hydrophobic and quasi-dry, whereas [BMI][PF_6] is more hygroscopic, and our simulations point to the importance of solvent humidity on the solvation of the free ions. Their first shell comprises, in addition to solvent anions, a few water molecules. Due to computer limitations, we did not explore less humid solutions, where some water should still coordinate to M^+, especially to the most hydrophilic cations (Na^+, Li^+), as found for the harder Sr^{2+},[26] UO_2^{2+}, or Eu^{3+} cations.[23] This should have a deep impact on, e.g., spectroscopic properties.[72] From the energy point of view, when the ionic liquid becomes more humid, the difference in Na^+/Cs^+ free energies of solvation increases in magnitude and comes closer to the value in water, as expected. The energy analysis also suggests that alkali cations should be more soluble in humid than in dry ILs.

Selectivity of Alkali Cation Extraction by the Calixcrown from Water to the Ionic Liquid. The calculations predict that **L** selectively extracts Cs^+ over Na^+, thus following the same trends with ILs as with traditional organic solvents. Intrinsically, however (i.e., in the gas phase), Na^+ interacts more strongly than Cs^+ with **L**,[31] and the extraction selectivity is mainly caused by the lower energy cost of desolvating Cs^+.

Water is more soluble in ionic liquids such as [BMI][PF_6] than in traditional solvents, and this influences the extraction selectivity. The presence of water in [BMI][PF_6] reduces the Cs^+/Na^+ extraction selectivity, from 9.7 kcal/mol in the dry liquid to 4.4 kcal/mol in the humid liquid, due to a lowering of the K^+/Na^+, Rb^+/K^+, and Cs^+/Rb^+ contributions. Thus, the presence of water is deleterious for an efficient separation of the Cs^+ cation.

Effect of the Nature of the Solvent Anion. For a given "naked" M^+ ion, there is little difference between the solvation in [BMI][PF_6] and in [BMI][Tf_2N] solvents, from the structural and energy points of view. A given $\mathbf{L}M^+$ complex also interacts similarly with the different solvents, leading to similar $\Delta G_{4/IL}$ energies when one cation is compared to the other. The differences in complexation and extraction free energies between the two dry solvents are quite small, indicating a weak influence of the nature of the solvent anion on the extraction and complexation selectivities. Other effects, e.g., hydrophobic/hydrophilic balance of the IL components and partioning to the aqueous phase, may be quite important however for, e.g., the efficiency of ion complexation or extraction, as well as the extraction mechanism.

Alkali Cation Complexation by the Calixcrown in a Given IL. To our knowledge, no study on alkali cation complexation in an ionic liquid has been reported yet. Detailed information on the solubility and status of alkali salts in ILs are also lacking. Our calculations are thus exploratory and predictive. Using a similar approach we correctly predicted the Cs^+/Na^+ selectivity by **L** as a function of its conformation,[27] and according to the present results, **L** should also complex selectively Cs^+ over Na^+ in a given IL. Comparing the two dry liquids, the selectivity should be more pronounced in [BMI][Tf_2N] than in [BMI][PF_6] ($\Delta\Delta G_c = 5.0$ kcal/mol), mainly due to the difference $\Delta G_{3/IL}$ between the solvation of the free K^+ and Na^+ cations. Indeed, K^+ is calculated to be more easily desolvated than Na^+ in the former than in the latter liquid. Similar FEP simulations have been reported for the M^+ complexation in a classical hydrophobic organic solvent (chloroform),[28] in which the selectivity was inversed (gas-phase-like behavior), i.e., Na^+ being preferred over Cs^+ (by 11.7 kcal/mol in the absence of a counterion and by 1.6 kcal/mol with one paired picrate counterion), mainly due to stronger interactions with the calixcrown.[31] In water, or in methanol, the selectivity was reversed, due to the desolvation of free M^+ ions,[31] i.e., ΔG_3 is smaller in magnitude than ΔG_4. Thus, despite their hydrophobic character, ILs behave more like

traditional polar solvents than like weakly polar or apolar ones, as far as the complexation selectivity is concerned.

Alkali Cations Transfer from Water to ILs. Chun et al. observed some transfer of uncomplexed alkali cations from an aqueous phase to ILs, contrary to traditional organic solvents where no transfer occurs.[12] The measured loading coefficients in the [BMI][PF_6] follow the relative "hydrophobicity" of the cations and are about 7% for the Cs^+, 5% for the Rb^+, 2% for K^+, and close to 0% for Na^+. These values are quite low and difficult to quantiatively reproduce by force field based FEP calculations. It is however quite gratifying to note that for [BMI]-[PF_6], we calculate a positive ΔG_e value (4.9 kcal/mol) indicating a better transfer of uncomplexed Cs^+, compared to Na^+. In the other liquids, ΔG_e is smaller (−0.2 kcal/mol) or null.

Conclusion

To summarize, the present MD and FEP study shows that Cs^+ should be best extracted by calixcrowns to ionic liquids, as well as complexed in a given IL, displaying marked analogies with extraction and complexation in classical organic solvents. The extraction results are in agreement with experiment, whereas the complexation results remain predictive. However, detailed analysis of the solvation patterns of M^+ ions — and to a lesser extent their complexes—reveals a number of specific features of these "green" media, particularly interesting from the technological as well as from the more fundamental point of view. Despite their polar character, they are found to behave as classical weakly polar molecular organic liquids as far as liquid−liquid extraction is concerned but more like polar liquids (water, alcohols) as far as the solvation of the M^+ cations and their complexation in a single phase is concerned.

Acknowledgment. The authors are grateful to IDRIS, CINES, Université Louis Pasteur, and PARIS for computer resources and to A. Chaumont, E. Engler, and R. Schurhammer for assistance.

Supporting Information Available: Tables S1−S12 and Figures S1−S3. This material is available free of charge via the Internet at http://pubs.acs.org.

References and Notes

(1) Casnati, A.; Pochini, A.; Ungaro, R.; Ugozzoli, F.; Arnaud, F.; Fanni, S.; Schwing, M. J.; Egberink, R. J. M.; de Jong, F.; Reinhoudt, D. N. *J. Am. Chem. Soc.* **1995**, *117*, 2767.

(2) Haverlock, T. J.; Bonnesen, P. V.; Sachleben, R. A.; Moyer, B. A. *J. Inclusion Phenom. Macrocyclic Chem.* **2000**, *36*, 21.

(3) Dozol, J. F.; Dozol, M.; Macias, R. M. *J. Inclusion Phenom. Macrocyclic Chem.* **2000**, *38*, 1.

(4) Bonnesen, P. V.; Delmau, L. H.; Moyer, B. A.; Leonard, R. A. *Solvent Extr. Ion Exch.* **2000**, *18*, 1079.

(5) Duchemin, C. R.; Engle, N. L.; Bonnesen, P. V.; Haverlock, T. J.; Delmau, L. H.; Moyer, B. A. *Solvent Extr. Ion Exch.* **2001**, *19*, 1037.

(6) Bonnesen, P. V.; Delmau, L. H.; Moyer, B. A.; Lumetta, G. J. *Solvent Extr. Ion Exch.* **2003**, *21*, 141.

(7) Engle, N. L.; Bonnesen, P. V.; Tomkins, B. A.; Haverlock, T. J.; Moyer, B. A. *Solvent Extr. Ion Exch.* **2004**, *22*, 611.

(8) Bazelaire, E.; Gorbunova, M. G.; Bonnesen, P. V.; Moyer, B. A.; Delmau, L. H. *Solvent Extr. Ion Exch.* **2004**, *22*, 637.

(9) Delmau, L. H.; Bonnesen, P. V.; Moyer, B. A. *Hydrometallurgy* **2004**, *72*, 9.

(10) Dai, S.; Ju, Y. H.; Barnes, C. E. *J. Chem. Soc., Dalton Trans.* **1999**, 1201.

(11) Visser, A. E.; Swatloski, R. P.; Reichert, W. M.; Griffin, S. T.; Rogers, R. D. *Ind. Eng. Chem. Res.* **2000**, *39*, 3596.

(12) Chun, S.; Dzyuba, S. V.; Bartsch, R. A. *Anal. Chem.* **2001**, *73*, 3737.

(13) Luo, H. M.; Dai, S.; Bonnesen, P. V.; Buchanan, A. C.; Holbrey, J. D.; Bridges, N. J.; Rogers, R. D. *Anal. Chem.* **2004**, *76*, 3078.

(14) Dietz, M. L.; Dzielawa, J. A. *Chem. Commun.* **2001**, 2124.

(15) Dietz, M. L.; Dzielawa, J. A.; Laszak, I.; Young, B. A.; Jensen, M. P. *Green Chem.* **2003**, *5*, 682.

(16) Stepinski, D. C.; Jensen, M. P.; Dzielawa, J. A.; Dietz, M. L. *Green Chem.* **2005**, *7*, 151.

(17) Nakashima, K.; Kubota, F.; Maruyama, T.; Goto, M. *Anal. Sci.* **2003**, *19*, 1097.

(18) Visser, A. E.; Jensen, M. P.; Laszak, I.; Nash, K. L.; Choppin, G. R.; Rogers, R. D. *Inorg. Chem.* **2003**, *42*, 2197.

(19) Jensen, M. P.; Neuefeind, J.; Beitz, J. V.; Skanthakumar, S.; Soderholm, L. *J. Am. Chem. Soc.* **2003**, *125*, 15466.

(20) Nakashima, K.; Kubota, F.; Maruyama, T.; Goto, M. *Ind. Eng. Chem. Res.* **2005**, *44*, 4368.

(21) Horwitz, E. P.; Kalina, D. G.; Diamond, H.; Vandergrift, G. F.; Schultz, W. W. *Solvent Extr. Ion Exch.* **1985**, *3*, 75.

(22) Chaumont, A.; Engler, E.; Wipff, G. *Chem. Eur. J.* **2003**, *9*, 635.

(23) Chaumont, A.; Wipff, G. *Inorg. Chem.* **2004**, *43*, 5891.

(24) Chaumont, A.; Wipff, G. *J. Phys. Chem. B* **2004**, *108*, 3311.

(25) Chaumont, A.; Wipff, G. *Phys. Chem. Chem. Phys.* **2005**, *7*, 1926.

(26) Vayssiere, P.; Chaumont, A.; Wipff, G. *Phys. Chem. Chem. Phys.* **2005**, *7*, 124.

(27) Lauterbach, M.; Wipff, G.; Mark, A.; van Gunsteren, W. F. *Gazz. Chim. Ital.* **1997**, *127*, 699.

(28) Lauterbach, M.; Wipff, G. In *Physical Supramolecular Chemistry*; Echegoyen, L., Kaifer, A. E., Eds.; Nato ASI Series; Kluwer Academic Publishers: Dordrecht, The Netherlands, 1996; Vol. 485, p 65.

(29) Varnek, A.; Wipff, G. *J. Mol. Struct.: THEOCHEM* **1996**, *363*, 67.

(30) Varnek, A.; Wipff, G. *J. Comput. Chem.* **1996**, *17*, 1520.

(31) Wipff, G.; Lauterbach, M. *Supramol. Chem.* **1995**, *6*, 187.

(32) Muzet, N.; Engler, E.; Wipff, G. *J. Phys. Chem. B* **1998**, *102*, 10772.

(33) Anthony, J. L.; Maginn, E. J.; Brennecke, J. F. *J. Phys. Chem. B* **2001**, *105*, 10942.

(34) Case, D. A.; Pearlman, D. A.; Caldwell, J. W.; Cheatham, T. E., III; Wang, J.; Ross, W. S.; Simmerling, C. L.; Darden, T. A.; Merz, K. M.; Stanton, R. V.; Cheng, A. L.; Vincent, J. J.; Crowley, M.; Tsui, V.; Gohlke, H.; Radmer, R. J.; Duan, Y.; Pitera, J.; Massova, I.; Seibel, G. L.; Singh, U. C.; Weiner, P. K.; Kollman, P. A. *AMBER7*; University of California: San Fransisco, CA, 2002.

(35) de Andrade, J.; Boes, E. S.; Stassen, H. *J. Phys. Chem. B* **2002**, *106*, 13344.

(36) Kaminski, G. A.; Jorgensen, W. L. *J. Chem. Soc., Perkin Trans.* **1999**, 2365.

(37) Margulis, C. J.; Stern, H. A.; Berne, B. J. *J. Phys. Chem. B* **2002**, *106*, 12017.

(38) Gough, C. A.; DeBolt, S. E.; Kollman, P. A. *J. Comput. Chem.* **1992**, *13*, 963.

(39) Lopes, J. N. C.; Deschamps, J.; Padua, A. A. H. *J. Phys. Chem. B* **2004**, *108*, 2038.

(40) Jorgensen, W. L.; Chandrasekhar, J.; Madura, J. D.; Impey, R. W.; Klein, M. L. *J. Chem. Phys.* **1983**, *79*, 926.

(41) Åqvist, J. *J. Phys. Chem.* **1990**, *94*, 8021.

(42) Cornell, W. D.; Cieplak, P.; Bayly, C. I.; Gould, I. R.; Merz, K. M., Jr.; Ferguson, D. M.; Spellmeyer, D. C.; Fox, T.; Caldwell, J. W.; Kollman, P. A. *J. Am. Chem. Soc.* **1995**, *117*, 5179.

(43) Allen, M. P.; Tildesley, D. J. *Computer Simulation of Liquids*; Clarendon Press: Oxford, 1987.

(44) Darden, T.; York, D.; Pedersen, L. *J. Chem. Phys.* **1993**, *98*, 10089.

(45) Berendsen, H. J. C.; Postma, J. P. M.; van Gunsteren, W. F.; DiNola, A.; Haak, J. R. *J. Chem. Phys.* **1984**, *81*, 3684.

(46) Engler, E.; Wipff, G. In *Crystallography of Supramolecular Compounds*; Tsoucaris, G., Atwood, J. L., Lipkowski, J., Eds.; Kluwer Academic Publishers: Dordrecht, The Netherlands, 1996; Vol. 480, p 471.

(47) Humphrey, W.; Dalke, A.; Schulten, K. *J. Mol. Graphics* **1996**, *14*, 33.

(48) Kollman, P. A. *Chem. Rev.* **1993**, *93*, 2395.

(49) Frisch, M. J.; Trucks, G. W.; Schlegel, H. B.; Scuseria, G. E.; Robb, M. A.; Cheeseman, J. R.; Montgomery, J. A.; Vreven, T.; Kudin, K. N.; Burant, J. C.; Millam, J. M.; Iyengar, S. S.; Tomasi, J.; Barone, V.; Mennucci, B.; Cossi, M.; Scalmani, G.; Rega, N.; Petersson, G. A.; Nakatsuji, H.; Hada, M.; Ehara, M.; Toyota, K.; Fukuda, R.; Hasegawa, J.; Ishida, M.; Nakajima, T.; Honda, Y.; Kitao, O.; Nakai, H.; Klene, M.; Li, X.; Knox, J. E.; Hratchian, H. P.; Cross, J. B.; Adamo, C.; Jaramillo, J.; Gomperts, R.; Stratmann, R. E.; Yazyev, O.; Austin, A. J.; Cammi, R.; Pomelli, C.; Ochterski, J. W.; Ayala, P. Y.; Morokuma, K.; Voth, G. A.; Salvador, P.; Dannenberg, J. J.; Zakrzewski, V. G.; Dapprich, S.; Daniels, A. D.; Strain, M. C.; Farkas, O.; Malick, D. K.; Rabuck, A. D.; Raghavachari, K.; Foresman, J. B.; Ortiz, J. V.; Cui, Q.; Baboul, A. G.; Clifford, S.; Cioslowski, J.; Stefanov, B. B.; Liu, G.; Liashenko, A.; Piskorz, P.; Komaromi, I.; Martin, R. L.; Fox, D. J.; Keith, T.; Al-Laham, M. A.; Peng, C. Y.; Nanayakkara, A.; Challacombe, M.; Gill, P. M. W.; Johnson, B.; Chen, W.; Wong, M. W.; Gonzalez, C.; Pople, J. A. *Gaussian 03*, revision B.05; Gaussian, Inc.: Pittsburgh, PA, 2003.

(50) Boys, S. F.; Bernardi, F. *Mol. Phys.* **1970**, *19*, 553.
(51) http://iris.theochem.uni-stuttgart.de/pseudopotentials/index.en.html.
(52) Wiberg, K. B.; Rablen, P. R. *J. Comput. Chem.* **1993**, *14*, 1504.
(53) Williams, D. B.; Stoll, M. E.; Scott, B. L.; Costa, D. A.; Oldham, W. J. *Chem. Commun.* **2005**, 1438.
(54) Bhatt, A. I.; May, I.; Volkovich, V. A.; Collison, D.; Helliwell, M.; Polovov, I. B.; Lewin, R. G. *Inorg. Chem.* **2005**, *44*, 4934.
(55) Chaumont, A.; Engler, E.; Wipff, G. *Inorg. Chem.* **2003**, *42*, 5348.
(56) Chaumont, A.; Wipff, G. *Phys. Chem. Chem. Phys.* **2003**, *5*, 3481.
(57) Chaumont, A.; Wipff, G. *Chem. Eur. J.* **2004**, *10*, 3919; Gaillard, C.; Billard, I.; Chaumont, A.; Mekki, S.; Ouadi, A.; Denecke, M.; Moutiers, G.; Wipff, G. *Inorg. Chem.* **2005**, *44*, 8335.
(58) Marcus, Y. *Ion Solvation*; Wiley-Interscience: Chichester, U.K., 1985.
(59) Liu, Z.; Huang, S.; Wang, W. *J. Phys. Chem. B* **2004**, *108*, 12978.
(60) de Andrade, J.; Boes, E. S.; Stassen, H. *J. Phys. Chem. B* **2002**, *106*, 3546.
(61) Morrow, T. I.; Maginn, E. J. *J. Phys. Chem. B* **2002**, *106*, 12807.
(62) Morrow, T. I.; Maginn, E. J. *J. Phys. Chem. B* **2003**, *107*, 9160.
(63) Shah, J. K.; Maginn, E. J. *Fluid Phase Equilib.* **2004**, *222*, 195.
(64) Martins, M. M.; Stassen, H. *J. Chem. Phys.* **2003**, *118*, 5558.
(65) Lynden-Bell, R. M.; Atamas, N. A.; Vasilyuk, A.; Hanke, C. G. *Mol. Phys.* **2002**, *100*, 3225.
(66) Hanke, C. G.; Lynden-Bell, R. M. *J. Phys. Chem. B* **2003**, *107*, 10873.
(67) Woodcock, L. V. *Chem. Phys. Lett.* **1971**, *10*, 257.
(68) Simon, C.; Cartailler, T.; Turq, P. *J. Chem. Phys.* **2002**, *117*, 3772.
(69) Velardez, G. F.; Alavi, S.; Thompson, D. L. *J. Chem. Phys.* **2004**, *120*, 9151.
(70) Lanning, O. J.; Madden, P. A. *J. Phys. Chem. B* **2004**, *108*, 11069.
(71) Born, M. *Z. Phys.* **1920**, *1*, 45.
(72) Billard, I.; Mekki, S.; Gaillard, C.; Hesemann, P.; Moutiers, G.; Mariet, C.; Labet, A.; Bünzli, J. C. G. *Eur. J. Inorg. Chem.* **2004**, 1190.